Journal of Medicinal Chemistry

Article

pubs.acs.org/jmc

Fragment-Based Design of Symmetrical Bis-benzimidazoles as Selective Inhibitors of the Trimethoprim-Resistant, Type II R67 Dihydrofolate Reductase

Dominic Bastien,[†] Maximilian C. C. J. C. Ebert,[†] Delphine Forge,[‡] Jacynthe Toulouse,[†] Natalia Kadnikova,[§] Florent Perron,[‡] Annie Mayence,[∥] Tien L. Huang,[∥] Jean Jacques Vanden Eynde,[‡] and Joelle N. Pelletier*[,†,§]

[†]Département de Biochimie, Université de Montréal, C.P. 6128, Succ. Centre-ville Montréal, Québec H3C 3J7, Canada

[‡]Laboratoire de Chimie Organique, Université de Mons-UMONS, 20 Place du Parc, B-7000 Mons, Belgium

[§]Département de Chimie, Université de Montréal, C.P. 6128, Succursale Centre-ville Montréal, Québec H3C 3J7, Canada

[∥]Division of Basic Pharmaceutical Sciences, Xavier University of Louisiana, 1 Drexel Drive, New Orleans, Louisiana 70125, United States

Supporting Information

ABSTRACT: The continuously increasing use of trimethoprim as a common antibiotic for medical use and for prophylactic application in terrestrial and aquatic animal farming has increased its prevalence in the environment. This has been accompanied by increased drug resistance, generally in the form of alterations in the drug target, dihydrofolate reductase (DHFR). The most highly resistant variants of DHFR are known as type II DHFR, among which R67 DHFR is the most broadly studied variant. We report the first attempt at designing specific inhibitors to this emerging drug target by fragment-based design. The detection of inhibition in R67 DHFR was accompanied by parallel monitoring of the human DHFR, as an assessment of compound selectivity. By those means, small aromatic molecules of 150−250 g/mol (fragments) inhibiting R67 DHFR selectively in the low millimolar range were identified. More complex, symmetrical bis-benzimidazoles and a bis-carboxyphenyl were then assayed as fragment-based leads, which procured selective inhibition of the target in the low micromolar range (K_i = 2−4 μM). The putative mode of inhibition is discussed according to molecular modeling supported by in vitro tests.

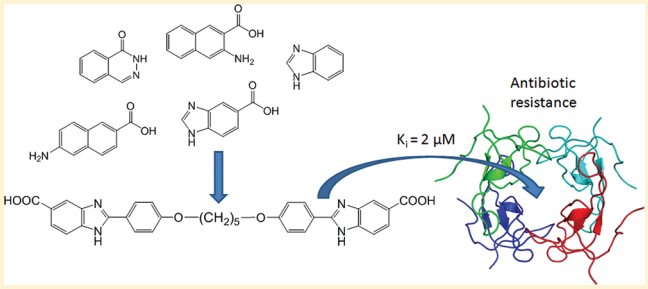

INTRODUCTION

Trimethoprim (TMP) has been used as an antibiotic worldwide for the past 50 years, frequently in combination with sulfamethoxazole.[1] Today, TMP remains a primary treatment of urinary *Escherichia coli* infections and is used to treat respiratory infections such as pneumonia. It has been used to treat sexually transmitted infections such as gonorrhea, but this has resulted in high TMP resistance.[2] As well, TMP with sulfamethoxazole shows potential for the treatment of tuberculosis,[2b] which causes an estimated 1.7 million deaths each year, and was recommended by the WHO in 2011 to reduce mortality due to opportunistic infections in adults living with HIV/AIDS.[3] In addition to medical use, TMP is also used for veterinary applications, including prophylactic use in porcine, bovine,[4] salmon,[5] and shrimp farming.[5,6] These result in large-scale environmental dissemination of the antibiotic,[7] which is inevitably accompanied by horizontal transfer of plasmids carrying multiple drug resistance genes to other microbes, including human pathogens.[5,8] As a result, there is a growing concern worldwide over the increased incidence in TMP resistance and its impact on the long-term effectiveness of this low-cost antibiotic.

TMP is a specific inhibitor of bacterial dihydrofolate reductases (DHFRs). DHFRs are oxidoreductases that catalyze the reduction of dihydrofolate (DHF) to tetrahydrofolate, using nicotinamide dinucleotide phosphate (NADPH) as a hydride-donating cofactor. DHFR is an essential enzyme for the synthesis of DNA precursors (purines, thymidylate) in all living cells, where it is chromosomally encoded and has been highly conserved throughout evolution.[9] Because of its essential role in cellular proliferation, DHFR is a central target in the control of proliferative diseases, including microbial infections. There are sufficient structural differences between human DHFR (hDHFR) and its microbial counterparts to allow for selective inhibition by compounds such as pyrimethamine and cycloguanyl, with high clinical efficacy.[10] TMP is such a selective inhibitor of microbial DHFRs; it binds to *E. coli* DHFR

Received: December 5, 2011
Published: March 16, 2012

dx.doi.org/10.1021/jm201645r | *J. Med. Chem.* 2012, 55, 3182−3192

approximately 4 orders of magnitude more tightly than it binds to hDHFR.[11] Among the mechanisms of TMP resistance that have been reported,[12] R-plasmid-encoded type II DHFR[13] constitutes an important health concern in both humans and livestock by sustaining bacterial proliferation.[14] Type II R67 DHFR catalyzes the same reaction as chromosomally encoded DHFR[15] albeit with a lower efficiency; yet, it evades the action of TMP, providing bacterial drug resistance.[13,16] Indeed, R67 DHFR is highly resistant to TMP, with IC_{50} and $K_i > 10^6$ fold higher than its chromosomal counterpart.[16,17] In contrast to the DHF substrate, TMP has no amide with which to H-bond with the Ile68 backbone. In addition, R67 DHFR has no carboxylate in its hydrophobic active site[18] and thus cannot form electrostatic interactions with the protonated TMP as seen in the chromosomal DHFR.[19] Indeed, R67 DHFR is genetically and structurally unrelated to chromosomal DHFRs, resulting in important structural differences that form the basis of its intrinsic TMP resistance. This enzyme is a homotetramer, where four identical protomers form a symmetrical active-site pore that binds a single DHF/NADPH pair for turnover.[19] The active-site cavity is a "binding hot-spot" of relatively low specificity that can bind two DHF or two NADPH molecules at once[17,19] and reduce some folate analogues.[15] This binding promiscuity runs counter the excruciatingly high binding stringency of hDHFR, which should allow for discovery of selective inhibitors of R67 DHFR that will not significantly inhibit hDHFR. Taken along with TMP, inhibitors of R67 DHFR would break TMP resistance granted by R67 DHFR.

Novobiocin, a DNA gyrase inhibitor, inhibits the activity of R67 DHFR as does congo red, a diazo dye.[17] Neither is specific to R67 DHFR; yet, they provide structural information relative to functional groups of interest in inhibitor design. In this work, we applied fragment-based inhibitor screening[20] to identify simple molecules that inhibit R67 selectively. While such small molecules may exhibit only a weak inhibitory effect due to their small size, they may form high quality interactions as expressed by the ratio of affinity to number of heavy atoms, or ligand efficiency (LE).[21] Inhibitory "fragments" allow the subsequent identification or design of more complex molecules sharing those substructures, which may display improved inhibition or other properties relevant to drug design. Molecules resulting from fragment-based design may require less optimization than their counterparts identified by more conventional high-throughput screening (HTS) campaigns, which may contain nondesirable functional groups.[21]

We seek molecules that bind within the active site in an effort to increase the likelihood of selectivity. Thus, screening for inhibition was carried out against a panel of approximately 100 simple compounds (or fragments) with a molecular weight of 150−250 g/mol. The fragments screened generally comprise cycles—often aromatic—and were generally of an overall elongated structure. Nitrogen and oxygen were preferred heteroatoms. While broader chemical diversity was also included, the above features were prioritized as they imitate features of the nicotinamide ring of NADPH and of the pteroyl ring of DHF, which are involved in binding to the center of the active-site cavity.[19] To restrict downstream efforts to molecules showing the best potential for selective inhibitor development, we screened the target bacterial R67 DHFR in parallel with human DHFR, which should be spared. Here, we report seven fragments that inhibit the R67 DHFR with an IC_{50} in the high micromolar to low millimolar range. Symmetrical bis-benzimidazole and bis-carboxyphenyl type compounds conserving features of the fragment molecules were subsequently tested for increased inhibition. Kinetic analysis and molecular modeling provided insight into the putative binding mode of these selective, micromolar inhibitors. Preliminary in vivo tests against adherent mouse fibroblast 3T6 cells revealed weak cytotoxicity.

MATERIALS AND METHODS

Materials. Dimethylsulfoxide (DMSO) was purchased from Fisher Scientific (Fair Lawn, NJ). The origin of the screened fragments is indicated in Table S1 in the Supporting Information. Solvents and reagents for synthesis are commercially available (Aldrich, Acros Organics, Fisher Scientific, Sigma Chemical Co.) and were used without further purification. DHF was synthesized from folic acid as described.[22] β-NADPH was purchased from Alexis biochemicals (San Diego, CA). Unless otherwise indicated, other reagents for enzyme expression and assays were from BioShop Canada Inc. (Burlington, ON).

Synthesis of Symmetrical Bis-benzamidine, Bis-benzimidazoles, and Bis-*p*-hydroxybenzoate. Compounds **8** and **9** were prepared and characterized following a known procedure.[23] Briefly, a mixture of 4-hydroxybenzaldehyde (5.12 g, 42 mmol), a dibromoalkane (C_4 or C_5) or dibromopropan-2-ol (20 mmol), and potassium carbonate (2.76 g, 20 mmol) in ethanol (10 mL) was heated under reflux for 8 h. After it was cooled, the precipitate was filtered and successively washed with water, ethanol, and ether. The bisbenzaldehyde was sufficiently pure to proceed to the next step. A mixture of the bisbenzaldehyde (3 mmol), sodium pyrosulfite (0.57 g, 3 mmol), 3,4-diaminobenzoic acid (0.91 g, 6 mmol), and water (3 mL) in ethanol (9 mL) was microwave irradiated (Biotage) for 15 min at 140 °C. After it was cooled, the precipitate was filtered and thoroughly washed with water, ethanol, and ether. Yields: **8**, 97%; **9**, 94%. The synthesis of compound **8b** was the same except for substitution of the diaminobenzoic acid with *ortho*-phenylenediamine (6 mmol).[23] The synthesis of compound **8a** has been reported;[24] however, a slightly modified version was performed. In short, a mixture of 4-hydroxybenzoic acid (0.69 g, 5 mmol), dibromopentane (7.5 mmol), potassium hydroxyde (0.84 g, 15 mmol), and water (1.5 mL) in ethanol (13.5 mL) was microwave irradiated for 20 min at 120 °C. After it was cooled, the precipitate was filtered and thoroughly washed with water, ethanol, and ether. Yield: 72%. Compounds were characterized by IR and ^{1}H NMR (see the Supporting Information).

Enzyme Purification. Recombinant type II R67 DHFR[18,25] with an N-terminal 6-histidine tag was overexpressed in *E. coli* BL21 containing plasmid pRep4 (Qiagen). Fresh overnight culture (3 mL) was added to Terrific Broth (1 L; 100 μg/mL ampicillin and 50 μg/mL kanamycin), and the flask was incubated at 37 °C and 250 rpm until OD_{600} reached approximately 0.7. Protein expression was induced by the addition of isopropyl β-D-1-thiogalactopyranoside (IPTG) to a concentration of 1 mM, with further incubation for 3 h. The cells were harvested by centrifugation (30 min, 2700*g*, 4 °C). The cell pellet was resuspended in 30 mL of lysis buffer (0.1 M potassium phosphate, 5 mM imidazole, pH 8.0), and the cells were disrupted by one passage through a cell disrupter (Constant Systems) adjusted to 27 kpsi. An additional 10 mL of buffer washed residual lysate through. Following centrifugation (30 min, 47500*g*, 4 °C) and filtration on a 0.22 μm filter, the supernatant was injected onto a 5 mL His-Trap HP cartridge at a flow rate of ∼1 mL/min using an Äkta FPLC (GE Healthcare). The column was washed with ∼12 column volumes (CV) of lysis buffer. A linear gradient (6 CV) of the same buffer + imidazole from 0 to 30 mM with a plateau (6 CV) at 30 mM was followed by a step to 300 mM imidazole for elution. Fractions containing R67 DHFR were identified according to activity assay and analysis on tricine-SDS-PAGE[26] and pooled for dialysis at 4 °C into to 0.1 M phosphate buffer, pH 8.0, using 3500 Da molecular weight cutoff dialysis tubing (Spectrum Laboratories). The protein concentration was determined using the Bradford protein assay (Bio-Rad) using bovine serum albumin (Bio-Rad) as a protein standard. Human

dx.doi.org/10.1021/jm201645r | J. Med. Chem. 2012, 55, 3182−3192

chromosomal DHFR was overexpressed in *E. coli* BL21 (DE3) and purified as described previously.[27]

Fragment-Based Inhibitor Screening against Purified Enzymes. Substrates were quantified by spectrophotometry in 50 mM potassium phosphate, pH 8.0 (ε_{340nm} = 6200 M^{-1} cm^{-1} for NADPH and ε_{282nm} = 28400 M^{-1} cm^{-1} for DHF). For inhibitor screening, the enzyme activity was determined by monitoring the depletion of NADPH and DHF at 340 nm ($\Delta\varepsilon_{340nm}$ = 12800 M^{-1} cm^{-1}) in 400 mM 4-(2-hydroxyethyl)-1-piperazineethanesulfonic acid (HEPES) buffer, pH 7.0, for R67 DHFR and 50 mM potassium phosphate, pH 8.0, for hDHFR. The high concentration of HEPES was required to offer adequate buffering in the presence of high concentrations of acidic or basic compounds, because the activity of R67 DHFR is exquisitely sensitive to pH changes.[28]

To provide adequate compound dissolution in a solvent system where both DHFRs retained appreciable activity, the maximal solubility of each test compound was determined in HEPES-buffered 10% DMSO. In that system, R67 DHFR retained 31% activity and hDHFR retained 17% activity, allowing reliable assessment of inhibition. For inhibition assays, each test compound was dissolved in neat DMSO and taken up in the reaction buffer containing the substrates, to a final DMSO concentration of 10%. For assay automation, testing was performed in a 96-well plate format with a reaction volume of 200 μL. When test compounds contributed to an excessive background absorbance at 340 nm, the activity was monitored in a volume of 100 μL to reduce the path length. Liquid handling was carried out using a BioMek NX automated workstation (Beckman Coulter), and data were collected with a Beckman DTX 880 plate-reader. Unless otherwise noted, final concentrations of NADPH and DHF were 50 μM. As a result, NADPH was at 30 × K_M^{NADPH}.[18] The inclusion of 10% DMSO weakens DHF binding, increasing the apparent K_M^{DHF} approximately 3-fold,[29] which is taken into account in all calculations. Here, DHF was at ~2 × K_M^{DHF}. These conditions provide a clear spectrophotometric signal in the case of uninhibited activity, without masking potential competitive inhibition. Reactions were initiated with the addition of 250 nM R67 DHFR. Initial rates (generally less than 10% substrate conversion) were determined. The determination of selectivity using hDHFR was performed under the same conditions except the buffer (see above). The concentration of hDHFR was 40 nM to allow measurement of initial rates while compensating for the higher turnover constant of hDHFR relative to R67 DHFR.

Determination of Binding and Kinetic Parameters. The IC_{50} values were determined with GraphPad Prism 5 using the log[inhibitor] vs response equation; K_i values were determined using the Cheng–Prusoff equation: $K_i = IC_{50}/([S]/K_M^{NADPH} + 1)$, assuming a competitive mode of inhibition.[30] K_M^{NADPH} used for the calculation was 1.6 ± 0.02 μM.[18] For determination of the mode of inhibition, the method of Dixon was used, in 50 mM potassium phosphate buffer, pH 7.0, with 10% DMSO. For inhibition relative to NADPH, DHF was held at 50 μM, and NADPH was at 5 or 80 μM (3- and 50-fold K_M^{NADPH}, respectively) and inhibitor over a range of concentrations spanning K_i. For inhibition relative to DHF, NADPH was held at 50 μM, and DHF was at 25 or 164 μM (~K_M^{DHF} and ~7-fold K_M^{DHF}) with inhibitor again spanning K_i. Initial rates were determined in 1 cm path-length cuvettes using a Cary 100 Bio UV–visible spectrophotometer (Agilent). For determination of binding stoichiometry, NADPH was held at 16 μM and DHF at 80 μM (10-fold K_M^{NADPH} and ~3-fold K_M^{DHF}, respectively) and titrated with increasing concentrations of **9**. Binding data were analyzed according to the Hill equation for inhibition: $\log[v_i/(v_0 - v_i)] = -n \log[I_i] + \log K_d$, where v_i is the velocity at inhibitor concentration $[I_i]$, v_0 is the noninhibited velocity, n is the Hill coefficient giving an indication of the number of binding sites, and K_d is the dissociation constant.

Molecular Docking Simulations. The crystal structure of a ternary complex of R67 DHFR (PDB file 2RK1[19]) was used for all docking simulations. The ligand 3D structures were drawn using ChemDraw 3D Pro 8.0. The geometry of the ligands was optimized using HyperChem 8.0.3 with the default settings. Docking simulations were run on a Dell XPS 1645 with an i7-720QM processor and 6 GB DDR3 running either Molegro Virtual Docker 4.0.0[31] or Autodock Vina 1.1.1.[32] For Molegro, the Moldock Score [Grid] scoring function was used. Grid resolution was 0.30 Å with a radius of 30. The search algorithm used was Moldock Optimizer, with default settings. The number of runs varied from 10 to 25, and the maximum iterations varied from 2000 to 10000. For Autodock Vina, the default settings were kept except the exhaustiveness parameter, which was increased from 8 to 25. Structural visualization was performed with Moldock.

Eukaryotic Cell Proliferation Assay. The cytotoxicity of compounds **8**, **8a**, **8b**, and **9** was evaluated using 3T6 fibroblast cells (kindly provided by the Laboratory of Biology and Embryology of the University of Mons-UMONS) in a eukaryotic cell viability test performed with the MTT (3-[4,5-dimethylthiazol-2-yl]-2,5-diphenyl-tetrazolium bromide) reduction assay.[33] MTT is a water-soluble tetrazolium salt that is cleaved into an insoluble purple formazan by the succinate dehydrogenase system of the mitochondrial chain, which is active only in live cells. 3T6 Fibroblasts are a permanent mouse embryonic fibroblast cell line. Cells were cultured in Dulbecco's modified Eagle's medium (DMEM) supplemented with 10% heat-inactivated fetal bovine serum (FBS) (Invitrogen), in a CO_2 incubator (37 °C, 5% CO_2). Trypsinized 3T6 cells (200 μL, 5 × 10^3 cells) were seeded in each well of a 96-well plate (except for the wells on the edge). Eight successive dilutions of each compound (in DMSO, Sigma Aldrich) were realized, from 200 to 0.05 μM. After 24 h of incubation, the culture medium was replaced with 200 μL of fresh medium containing the same compound dilutions. Culture medium (200 μL) was also added to the cell growth control rows while the solvent control wells received 200 μL of the relevant mixture of DMSO and culture medium. Blanks (no cells) received the same mixture. After a further 48 h of incubation, the cells were carefully washed with PBS, and 100 μL of fresh culture medium were added into each well. MTT (100 μL) (In vitro toxicology assay kit, MTT based, Sigma Aldrich) was then added to all wells and incubated for 3 h. The reaction was stopped by adding MTT solubilization reagent. After overnight incubation at 37 °C, the formazan dye was quantified with a microplate reader (Thermo Labsystems Multiskan Ascent 354) using a test wavelength of 540 nm and a reference wavelength of 690 nm. Eight concentrations of each test compound (0.05–200 μM) were verified in triplicate. The % inhibition of cell proliferation was calculated as follows: % IC = 100 − [corrected mean OD sample ×100/corrected mean OD solvent controls], where % IC = % inhibition of cell proliferation, and corrected mean OD sample/solvent = mean $OD_{540-690}$ of samples/controls − mean $OD_{540-690}$ of blanks. For each compound, the % inhibition of activity was plotted against the compound concentration scale. The concentration inhibiting 50% of cell proliferation (IC_{50}) was the x-axis value corresponding to one-half of the maximal absorbance value.

RESULTS AND DISCUSSION

Fragment-Based Inhibitor Screening of R67 DHFR. To date, two nonspecific micromolar inhibitors of R67 DHFR have been reported: novobiocin (K_i = 60 μM), a DNA gyrase inhibitor, and congo red, a diazo dye (K_i = 2 μM).[17] Their structural differences relative to the other known micromolar ligands of R67 DHFR, namely, the DHF substrate and NADPH cofactor, as well as the loose substrate specificity of the enzyme,[15] immediately suggest that the active site is amenable to fragment-based inhibitor design. Accordingly, we selected a panel of small organic compounds (fragments) for inhibitor screening, based on structural similarity to the moieties of the substrate and cofactor, which bind deepest in the active-site pore.[19] Approximately 100 commercially available compounds that share some chemical features of the DHF substrate pteroyl group or NADPH cofactor nicotinamide ring were screened for selective inhibition of R67 DHFR relative to hDHFR (Table S1 in the Supporting Information). Because the compounds are simple and possess a low molecular weight (150–250 g/mol),

dx.doi.org/10.1021/jm201645r | J. Med. Chem. 2012, 55, 3182–3192

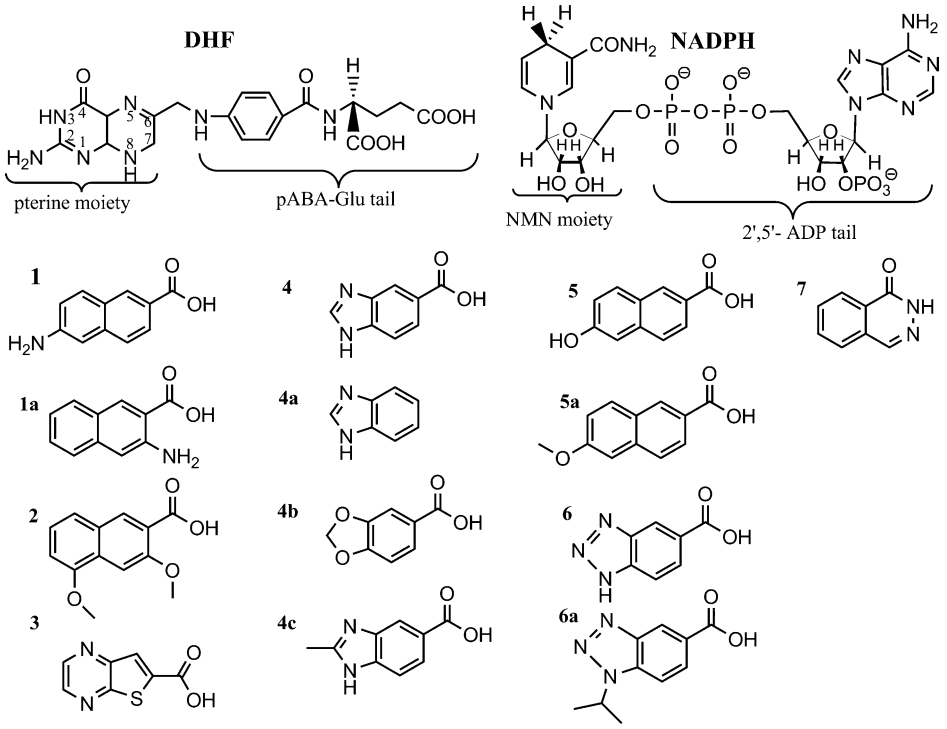

Figure 1. Structures of the weak inhibitor fragments and their inactive analogues. Structures of the DHF substrate and NADPH cofactor are provided as a reference. Compounds: **1**, 6-aminoisonaphthoic acid; **1a**, 3-aminoisonaphthoic acid; **2**, 3,5-dimethoxyisonaphthoic acid; **3**, thieno[2,3-*b*]pyrazine-6-carboxylic acid; **4**, 1*H*-benzimidazole-5-carboxylic acid; **4a**, benzimidazole; **4b**, piperonylic acid; **4c**, 2-methyl-1*H*-benzimidazole-5-carboxylic acid; **5**, 6-hydroxy-2-naphthoic acid; **5a**, 6-methoxy-2-naphthoic acid; **6**, 1*H*-benzotriazole-5-carboxylic; **6a**, 1-methylethyl-1*H*-benzotriazole-5-carboxylic acid; and **7**, 1(2*H*)-phthalazinone. No inhibition was observed up to 5 (**1a** and **5a**), 10 (**4c** and **6a**), or 30 mM (**4a** and **4b**), which are the highest concentrations that could be tested due to constraints of poor solubility and high absorbance.

no strong inhibition was expected. Hence, they were tested for inhibition at mM concentrations. Figure 1 illustrates compounds **1**–**7**, which provided inhibition with an IC_{50} in the low- to midmillimolar range (Table 1), as well as some structural analogues, which provided no inhibition.

Table 1. Inhibition of R67 DHFR and hDHFR by Fragments 1–7[a]

compd	IC_{50} (mM)	K_i (μM)	relative activity hDHFR (%)[b]	LE (kcal)
1	1.7 ± 0.3	51 ± 9	14 ± 13	−0.32
2	1.8 ± 0.4	55 ± 14	14 ± 4	−0.32
3	2.0 ± 1.3	61 ± 41	37 ± 9	−0.48
4	2.6 ± 1.4	80 ± 42	75 ± 5	−0.47
5	6.1 ± 2.3	190 ± 71	13 ± 2	−0.36
6	8.4 ± 2.6	260 ± 80	69 ± 13	−0.41
7	17 ± 1.7	530 ± 54	97 ± 3	−0.32

[a]Values are given as the average ± standard deviation from the mean. [b]Compounds were tested at the highest possible concentration (**1** = 2.5 mM, **2** and **3** = 5 mM, **4** and **5** = 10 mM, and **6** and **7** = 30 mM), taking into account constraints due to poor solubility and high absorbance.

Compounds **1**, **2**, and **5** possess a naphthalene core substituted with a carboxylic acid but are differently functionalized. Despite the differences between the 6-amino group of **1** and the 2,5-dimethoxy substitution of **2**, their IC_{50} values are unchanged (1.7 and 1.8 mM for compounds **1** and **2**, respectively). However, with the amino group at position 2 (**1a**), no inhibition was observed. The vicinal carboxylate and amino groups of **1a** have the potential for intramolecular H-bonding, which would modulate the electronic effect of these functional groups relative to **1**. Compound **5** is hydroxylated at position 6 and shows inhibition similar to **1** and **2** (IC_{50} = 6.1 mM), while a 6-methoxy substituent abrogated inhibition (**5a**). These results suggest the positive contribution of a hydrophilic substituent at C5 or C6 of the naphthoic acid, opposite the carboxylic acid, although different substituents modulate the inhibitory activity of the naphthoic acid framework.

Compound **3**, a thienopyrazine framework substituted with a carboxylic acid, inhibited R67 DHFR with an IC_{50} of 2.0 mM, in the same range as the similarly substituted benzimidazole **4** (IC_{50} = 2.6 mM) and the carboxylate-substituted benzotriazole **6** (IC_{50} = 8.4 mM). Benzimidazole (**4a**) gave no inhibition, confirming the contribution of the carboxylic acid substitution to inhibition. Changing the aromatic diimino ring to a dioxole ring (compound **4b**) prevented inhibition, suggesting the importance of aromaticity and/or polarity of heteroatoms. It is not clear why an additional methyl substituent at C6 of the acid-substituted benzimidazole (**4c**) abrogated inhibition, since it will be shown below that C6 was used to build fragment **4** into a more complex inhibitor (vide infra). An additional isopropyl at N5 of the acid-substituted benzotriazole (**6a**) prevented inhibition, indicating that additional bulk or hydrophobicity at positions opposite the carboxylic acid substituent are to be avoided. The only inhibitor identified that carried no carboxylic acid substituent was **7**, the weakest inhibitor with IC_{50} = 17 mM.

By way of fragment screening, we thus identified several weak inhibitors of R67 DHFR. All are hydrophobic and aromatic and possess a carboxylic acid (except the weaker inhibitor **7**). The

dx.doi.org/10.1021/jm201645r | *J. Med. Chem.* 2012, 55, 3182–3192

positions opposite the carboxylic acid modulate the activity of the compound and could be targeted to improve these inhibitors.

To direct inhibitor development toward selectivity for R67 DHFR while sparing human DHFR (hDHFR), we tested these seven fragments against hDHFR. Compounds **4** and **6** displayed good selectivity: at 3 × IC_{50}, approximately 80% of hDHFR activity remained. Compound **7** did not affect the activity of the hDHFR up to 30 mM (2 × IC_{50}). However, compounds **1**, **2**, **3**, and **5** inhibited nonselectively: at <2 × IC_{50}, these compounds strongly inhibited hDHFR. Although **4** and **6** were not the most potent, they showed a good selectivity for R67 DHFR, and they have a good LE, where LE is ΔG of binding (calculated from K_i) divided by the number of heavy atoms in the molecule (Table 1). LE indicates how efficiently a compound binds to its target, relative to its molecular weight. In a recent example, careful optimization of millimolar fragments with a LE of −0.30 kcal and less provided nanomolar inhibitors.[21] Fragment **4** possesses a good potency, selectivity, and a LE of −0.47 kcal; it was thus selected as a basis for development of a more potent inhibitor.

Inhibition of R67 DHFR by Symmetrical Polyaromatic Molecules. As mentioned above, novobiocin (K_i = 70 μM) and congo red (K_i = 2 μM) (Figure 2) are the only two known R67 DHFR inhibitors, and neither is specific to R67 DHFR. Both structures are elongated and possess substituted aromatic rings. Notably, the more potent congo red is symmetrical, with a negatively charged substituent on each extremity and a central hydrophobic linker. R67 DHFR possesses a symmetrical and mostly hydrophobic active site,[25] the center of which holds the reactive groups of the DHF substrate and NADPH cofactor. Upon binding of DHF and NADPH, Lys32 from the four DHFR protomers—which lie at the mouth of the active-site channel—bind to the negatively charged DHF carboxylates and NADPH phosphates.[34] We hypothesized that the sulfites of congo red and carboxylic acid substituents of fragments **1**−**6** interact with these lysines or with the neighboring Lys33 (from each of the four protomers), which lie further outside of the active-site channel. Thus, we tested inhibition with symmetrical compounds constituted of two fragments **4** symmetrically connected with a semirigid hydrophobic linker (yielding **8**) or a shorter, slightly more hydrophobic linker (yielding **9**) (Figure 2).

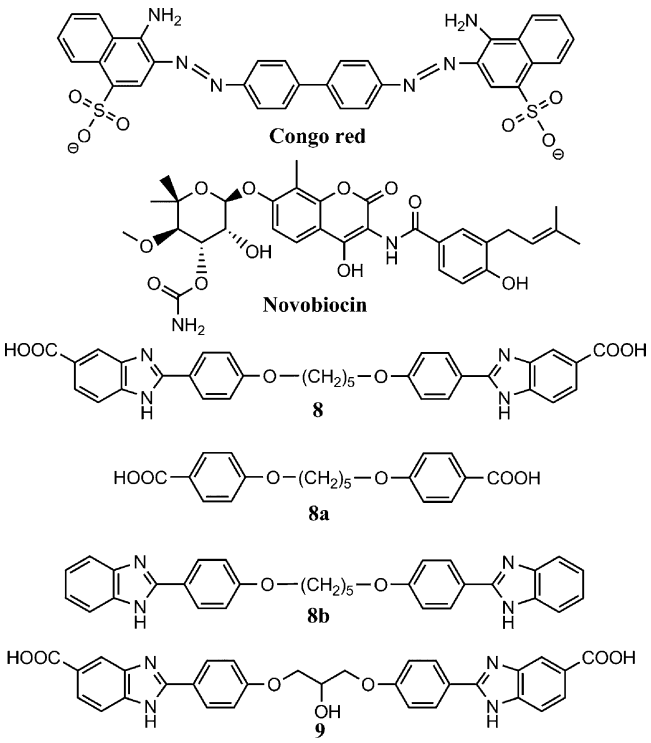

Figure 2. Structures of the R67 DHFR inhibitors and their inactive analogues. Congo red and novobiocin are nonspecific inhibitors of R67 DHFR. Compounds: **8**, 2,2′-[1,5-pentanediylbis(4-oxyphenylene)]-bis-1*H*-benzimidazole-5-carboxylic acid; **8a**, 4,4′-[1,5-pentanediyl-(oxy)]-bisbenzoic acid; **8b**, 2,2′-[1,5-pentanediylbis(4-oxyphenylene)]-bis-1*H*-benzimidazole; and **9**, 2′-(4,4′-(2-hydroxypropane-1,3-diyl)-bis-(4-oxyphenylene)-bis-1*H*-benzimidazole-5-carboxylic acid.

We observed an improvement in potency, with IC_{50} of 64 and 130 μM for compounds **8** and **9**, respectively (as compared to 2.6 mM for **4**) (Table 2 and Figure S1 in the Supporting Information). To gain insight into the structure−activity relationship (SAR), we tested two analogues of **8** (**8a** and **8b**). Removing the benzimidazole moiety from **8** (yielding **8a**) provided no inhibition up to the highest concentration tested (1 mM). Removing the carboxylic acid from the benzimidazole moiety (yielding **8b**) reduced the potency: at 300 μM, more than 60% of R67 activity remained, demonstrating that the carboxylic acid functions are important contributors to binding. Nonetheless, lack of inhibition with **8a** demonstrated that carboxylic acids alone are not sufficient for binding to R67 DHFR. To verify if the selectivity of the inhibitors was conserved, we tested inhibitors **8** and **9** against hDHFR (Table 2). No inhibition of hDHFR was observed up to the highest concentrations tested (400 μM **8**, 1 mM **8a**, 300 μM **8b**, and 1 mM **9**).

Table 2. Inhibition of R67 DHFR and hDHFR by Symmetrical Compounds 8 and 9[a]

compd	IC_{50} (μM)	K_i[b] (μM)	relative activity hDHFR (%)[c]	LE (kcal)
8	64 ± 11	2.0 ± 0.3	95 ± 11	−0.18
8a	≥1000	ND	100 ± 1	ND
8b	≥300	ND	110 ± 14	ND
9	130 ± 11	4.0 ± 0.3	95 ± 10	−0.18

[a]Values are given as the average ± standard deviation from the mean. ND, not determined. [b]K_i was calculated from IC_{50} values. [c]Compounds were tested at the highest possible concentration (**8** = 400 μM, **8a** = 1 mM, **8b** = 300 μM, and **9** = 1 mM), taking into account constraints due to poor solubility and high absorbance.

Overall, starting from fragment **4**, which gave a millimolar range IC_{50} and a LE of −0.47 kcal (Table 1), we identified two selective inhibitors of R67 DHFR (**8** and **9**), which showed IC_{50} 300−600-fold lower, in the micromolar range. Compounds **8** and **9** possess a LE of −0.18 kcal (Table 2) and thus bind less efficiently relative to their molecular weight than the precursor fragment **4**. This illustrates that they are poorly optimized compounds. Thus, inhibitors **8** and **9** provide a starting point to develop potent and selective inhibitors against R67 DHFR.

Inhibition Is Competitive. To understand the binding mode of the symmetrical inhibitors to their target, the mode of inhibition of **8** toward R67 DHFR was determined according to the method of Dixon, by performing inhibition at varying NADPH and inhibitor concentrations.[35] Figure 3 illustrates that

dx.doi.org/10.1021/jm201645r | J. Med. Chem. 2012, 55, 3182−3192

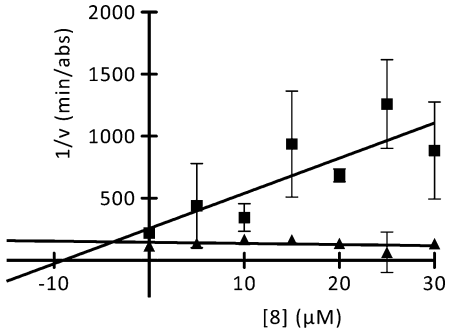

Figure 3. Dixon plot for the determination of type of inhibition of R67 DHFR by **8**, relative to the NADPH cofactor. The reciprocal rates of DHFR activity were plotted as a function of inhibitor concentration. DHF substrate was held at 50 μM. NADPH cofactor was held at 5 (3 × K_M^{NADPH}; ■) or 80 μM (50 × K_M^{NADPH}; ▲). Values are given as the mean ± standard deviation for triplicate results. The intercept of the two slopes gave K_i (**8**) = 4.2 μM.

8 is a competitive inhibitor, with K_i = 4.2 μM against the cofactor NADPH. This value is consistent with that calculated from IC_{50} (Table 2). Compound **8** showed similar results toward the substrate DHF, with a K_i of 9.7 μM (Figure S2 in the Supporting Information). The competitive nature of the inhibition with respect to both the substrate and the cofactor is consistent with the inhibitor binding within the active-site cavity.

Docked Model of Inhibitor Binding to R67 DHFR. To help direct future efforts in improving the inhibitors, compounds **8**, **8a**, **8b**, and **9** were docked into the crystal structure of R67 DHFR (2RK1[19]). Each of the four protomers of the R67 DHFR homotetramer plays a different role when a molecule binds in the active site, thus breaking the tetramer's symmetry.[36] For clarity, we will refer to residues according to their chain identity (protomer^a to protomer^d), as required. Figure 4A–C shows that R67 DHFR forms a symmetrical homotetramer where the active site lies within the central channel. The entrances to the pore are lined with the positively charged Lys32 and Lys33, each contributed by symmetry-related protomers (i.e., protomer^a and protomer^d or protomer^b and protomer^c) to provide four lysines at each entrance to the pore (Figure 4C). They serve to bind and orient the phosphates of the cofactor NADPH and the carboxylates of the substrate DHF.[34] The NADPH nicotinamide ring and the DHF pteroyl group, which contain the hydride donor and acceptor, respectively, meet at the mostly hydrophobic center of the pore for reactivity, where Gln67, Ile68, and Tyr69 are key binding residues. In particular, Gln67 forms a H-bond network with Tyr69, providing a molecular "clamp" that holds the substrates in place.[19] The unusual symmetry of the active-site pore and its binding promiscuity,[15] in addition to the cooperativity of NADPH and DHF binding,[37] increase the difficulty of obtaining meaningful docking results. Docking to the apo-form of the crystallized ternary complex was shown to give results that were inconsistent with that complex,[38] although docking of one ligand in the presence of the second has proven more reliable.[38,39] Nonetheless, we assume that inhibitor binding follows the simplest model of binding to the apoenzyme—this is consistent with inhibition being competitive against both DHF and NADPH, although it does not necessarily demonstrate it. DHF binding was not deemed a meaningful control because only its pterin ring has been resolved. We thus conducted a docking control on the apoenzyme using the ligand NADPH. In the five poses corresponding to the best docking scores, the nicotinamide moiety and the three phosphates were roughly well localized, although the adenine ring made contacts with different faces of the channel. Thus, the docking of NADPH to the apoenzyme could not be directly compared to the bound conformer in the crystallized ternary complex but served as a guide for relative docking scores of the inhibitors.

Compounds **8**, **8a**, **8b**, and **9** were docked onto R67 DHFR using Molegro Virtual Docker. The docking scores are reported in Table 3, with NADPH as the reference compound. K_M^{NADPH} is 1.6 μM[18] (for the ternary complex). Its docking score (for the binary complex) was −190, where the score is a dimensionless unit estimating the binding energy. The scores for inhibitors **8** and **9** were similar, at −190 and −185, respectively, consistent with their K_i (for **8**: calculated from IC_{50} = 2.0 μM, experimentally determined = 4.2 μM; for **9**: calculated from IC_{50} = 4.0 μM), which are similar to K_M^{NADPH}. Compounds **8a** and **8b** provided weaker scores of −109 and −156, respectively, reflecting the poor inhibition properties that were apparent in their respective IC_{50} values.

Typical poses obtained for these compounds are shown in Figure 4D–K. Interestingly, each of the four R67-bound inhibitors was predicted to adopt a U shape, with stacking of the symmetry-related aromatic moieties. The aromatic stacking would fill the volume of the cavity in a manner similar to the juxtaposition of the NADPH and DHF during the native reaction. This proposed binding mode is consistent with the symmetry of the tetrameric active site, where each arm of the inhibitor forms similar contacts with symmetry-related residues of the enzyme (i.e., protomer^a and protomer^d). Furthermore, it is consistent with the hydrophobic nature of the center of the active site, which would disfavor "threading" of the charged extremity of any of these compounds through the active-site channel. Overall, it is consistent with a competitive mode of inhibition. Specific features of the predicted mode of binding are discussed below.

Compound **9** has the most hydrophilic central spacer; interestingly, the docked model predicts that **9** is deeply bound within the active site, where the glycerol spacer appears to strongly interact with the backbone of Ile68^c (Figure 4J,K). Ile68 is proposed to provide recognition of the carboxamide on the nicotinamide ring and the amide on the pteridine ring.[19] As a result, the benzene and benzimidazole would form van der Waals interactions with the central hydrophobic pocket. The central pocket would be fully occupied, as shown in Figure 4K, where the docked molecule is predicted to traverse the center of symmetry of the enzyme. Lys32^a has the potential to form an electrostatic bond with a benzimidazole carboxylate (Figure 4J), consistent with its role in binding the NADPH phosphate or the DHF glutamate tail to orient these molecules in the active site. Moreover, in the model, Gln67^a H-bonds with the benzimidazole moiety, and Ser65^b H-bonds with the terminal carboxylate.

The docked model of compound **8** (Figure 4D,E) was bound less deeply within the hydrophobic pocket, although it was also predicted to traverse the lengthwise center of symmetry of the channel. Interactions with the backbone of Ile68 were lost due to the more hydrophobic nature of the spacer, but interactions with Gln67^b and Gln67^c were gained. This position allows the terminal carboxylates to H-bond with residues Thr51^a, Tyr46^a, and Ala36^a, in addition to allowing electrostatic interaction with Lys32^d. Compound **8b** (Figure 4H,I) differs from **8** by its lack

dx.doi.org/10.1021/jm201645r | J. Med. Chem. 2012, 55, 3182–3192

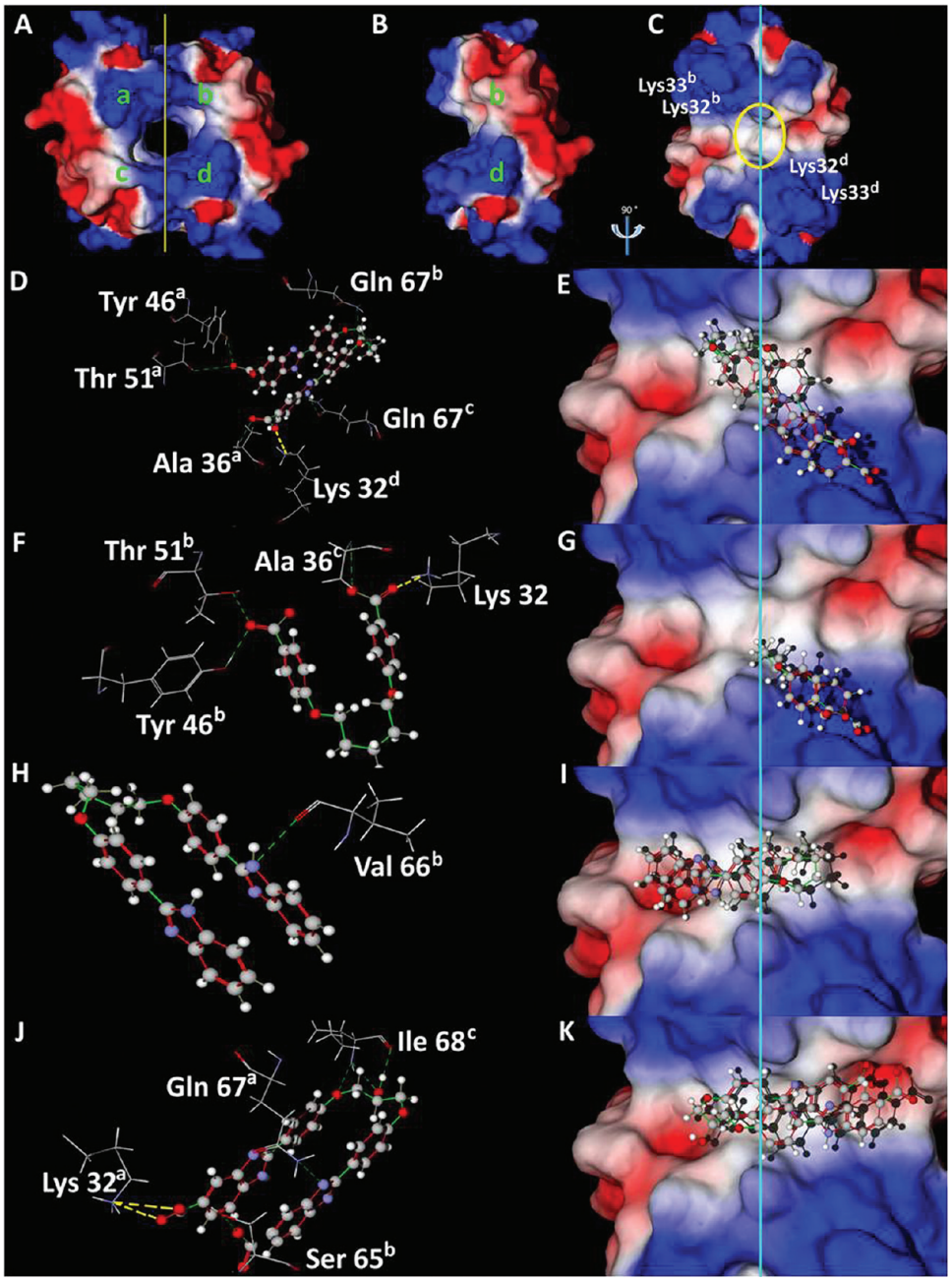

Figure 4. Docking of **8**, **8a**, **8b**, and **9** R67 DHFR using Molegro Virtual Docker. (A) R67 DHFR is shown as an electrostatics surface with the basic, acidic, and hydrophobic regions shown in blue, red, and white, respectively, and protomers labeled a–d. (B) Two protomers are shown, where the tetramer was split as indicated in panel A. (C) A 90° counter-clockwise rotation of panel B, revealing the largely hydrophobic active-site cavity (circled). (D–K) Docking of **8**, **8a**, **8b**, and **9**. (D and E) Docking of **8**, (F and G) **8a**, (H and I) **8b**, and (J and K) **9**. The left-hand panels show putative contacts formed, with the compound in ball-and-stick representation and the residues of R67 DHFR in sticks representation. Hydrogen, carbon, nitrogen, and oxygen are in white, gray, blue, and red balls, respectively. Red and green bonds represent the nonrotatable and rotatable bonds, respectively, as defined for docking experiments. Yellow and green dashed lines represent electrostatic bonds and H-bonds, respectively. The right-hand panels show the same result, with the enzyme active site oriented as in panel C. The vertical blue line indicates the center of symmetry for the axis that runs lengthwise through the binding channel.

of terminal carboxylates on the benzimidazole moieties. Compound **8b** was also deeply docked in the active site. The interactions with Thr51, Tyr46, Ala36, and Lys32 predicted with **9** were lost with **8b** due to the lack of the carboxylates. This result is consistent with the IC_{50} for **8b**, which is at least 5-fold higher than **8**. Compound **8a** (Figure 4F,G) differs from **8** and **9** by its lack of benzimidazole moieties. In the docked model, the terminal carboxylates formed the same H-bonding and electrostatic interactions observed with **8**, which suggests that the benzimidazole moiety is not essential to the formation of these interactions. Putative interactions with Gln67 and Ile68 were lost as a consequence of the loss of the benzimidazole heteroatoms and the replacement of the glycerol moiety by pentane, which could explain the lower docking score and the lack of in vitro inhibition. Compound **8a** was also the least deeply docked into the active site.

Docking with Autodock Vina afforded essentially superimposable results (Figure S3 in the Supporting Information):

dx.doi.org/10.1021/jm201645r | *J. Med. Chem.* 2012, 55, 3182–3192

Table 3. Docking of NADPH and 8, 8a, 8b, and 9 to R67 DHFR

compd	Moldock score
NADPH	−190
8	−190
8a	−109
8b	−156
9	−185

the inhibitors folded into a U shape, slipping the center of the molecule deep into the active-site channel with the carboxylates generally held by Lys32; Tyr46, Thr51, and Ser65 also participated in carboxylate binding (not shown). Similar interactions were predicted with Gln67, Ile68, and Tyr69 as when docking with Molegro.

While these models suggest that intramolecular stacking occurs upon binding, this may result from limitations of the docking algorithms used. Specifically, docking algorithms dock a single molecule of test compound at a time. Thus, the U shape that we observed may reflect a virtual solution to maximize molecular packing within the active-site tunnel. An alternative docking method of compounds **8**, **8a**, and **9** has shown a linear mode of binding (Hogue, H., Purisima, E., and Sulea, T. Personal communication). In that case, the molecule threads through the length of the active-site pore, forming essentially the same contacts as in the U shape, except that the two R67 DHFR protomers that it interacts with are on opposite ends of the channel (thus interacting with protomer[a] and protomer[c] rather than protomer[a] and protomer[d]). Indeed, it is possible that two molecules of a given compound bind simultaneously, laying flat on top of each other, thus maximizing the contacts with the large active-site tunnel. That mode of binding remains consistent with the hydrophobicity of the tunnel, with the putative role of the 4-fold Lys32 residues in binding the inhibitors' carboxylates, with the volume occupied by the stacking of the natural DHF substrate and NADPH cofactor and provides a more entropically favored solution to binding; threading of the terminal carboxylate through the hydrophobic active site may be promoted by the water molecules known to populate the active-site pore.[19] Attempts were made to soak inhibitor **9** into R67 DHFR crystals that were obtained using a recently described crystallization protocol.[25] A change in the electron density was observed in the active-site pore in the presence of **9** relative to the apo structure of R67 DHFR (Yachnin, B., Colin, D., Berghuis, A. Personal communication). Unfortunately, because the pore lies on the crystallographic symmetry axes, combined with the fact that the ligand did not appear to be present at full occupancy, it proved impossible to interpret the electron density. From what could be seen, the density was not consistent with the U-shaped conformation of compound **9** as suggested by the dockings results, but the poor quality of the electron density precludes drawing conclusions on the actual bound conformation of the inhibitor.

Notwithstanding the precise mode of binding, symmetry appears to play a key role in binding and selectivity for R67 DHFR. The proposed interaction of terminal carboxylates with Lys32, Thr51, Tyr46, or Ala36 may be modulated by the distance between the carboxylate and the hydrophobic pocket as observed by comparing docked models of **8** and **9**. Interaction with the backbone of Ile68 and Val66 may be promoted by a heteroatom near the hydrophobic pocket.

Binding Stoichiometry. As mentioned above, if the inhibitor molecules **8** or **9** were to bind to the active site in a linear conformation, it is conceptually possible for two molecules to bind simultaneously. In contrast, the model of the U-shaped conformation of bound **8** or **9** would not allow this (Figure 4). We examined binding stoichiometry by performing competitive inhibition under conditions appropriate for determining a Hill coefficient. As shown in Figure 5 (inset),

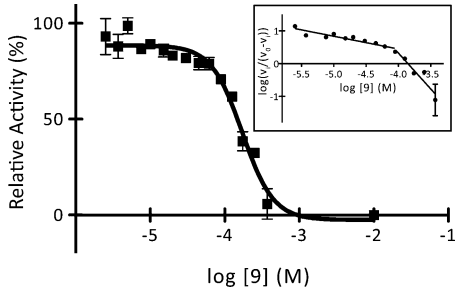

Figure 5. Hill plot for the determination of the stoichiometry of binding of compound **9** to R67 DHFR. Semilogarithmic representation of the relative activity vs the inhibitor concentration. DHF substrate was held at 80 μM (~3 × K_M^{DHF}) and NADPH cofactor at 16 μM (10 × K_M^{NADPH}). The calculated Hill coefficient was 2.1 ± 0.3. The inset represents the corresponding double logarithmic Hill plot. The best fit to the data does not follow a single straight line but is a composite of two straight lines with different slopes. The apparent Hill coefficients were 0.39 ± 0.06 for low inhibitor concentrations and 2.2 ± 0.4 for high inhibitor concentrations. Values are given as the mean ± standard deviation for triplicate results.

the Hill plot with **9** shows a clear inflection, consistent with more than one inhibitor molecule binding to the target.[40] The apparent Hill coefficients obtained are 0.39 ± 0.06 at low inhibitor concentrations and 2.2 ± 0.4 at high inhibitor concentrations, while the Hill coefficient obtained upon plotting in semilogarithmic format is 2.1 ± 0.3 (Figure 5). These values are consistent with R67 having the potential to bind more than one inhibitor molecule simultaneously.[40] However, there was no evidence of binding cooperativity according to a replot of reaction rate relative to inhibitor concentration (not shown).[40]

These results support binding of the inhibitors in a linear mode, where it is sterically possible to stack two molecules into the active site, rather than the U-shaped docked models (Figure 4), where inhibitors **8** and **9** both cross the center of symmetry of the active site such that it would not be possible to fit in two molecules simultaneously. It should be noted that a further sterically plausible binding mode would be for one molecule of inhibitor to bind in a linear mode concurrently with one molecule of NADPH or DHF. We attempted to verify this according to fluorescence binding measurements, but compounds **8** and **9** both gave rise to strong fluorescence plagued by intense quenching at the relevant micromolar concentrations.

In Vivo Assays. Determination of the minimum inhibitory concentration (MIC) for compounds **8** and **9** was attempted using *E. coli* XL1-Blue expressing DHFR R67 in minimum media (M9) containing 50 μg/mL of TMP (to inhibit the native, chromosomal *E. coli* DHFR). Bacterial growth was not inhibited up to 1 mM **8** or **9** (maximal concentration tested; data not shown), suggesting that these compounds do not penetrate into *E. coli*. We considered testing esterified versions

dx.doi.org/10.1021/jm201645r | J. Med. Chem. 2012, 55, 3182−3192

of the inhibitors to increase their permeability in microbial cells, but their solubility became too low to allow testing at meaningful concentrations. Nonetheless, **8b** has an antiproliferative effect on *Leishmania donovani*, *Pneumocystis carinii*, *Plasmodium falciparum*, and *Trypanosoma brucei rhodesiense*, although their mode of action has not yet been determined.[23] Compounds **8**, **8a**, **8b**, and **9** exhibited only weak cytotoxicity against adherent mouse fibroblast 3T6 cells with the exception of compound **8b**, which exhibited an IC_{50} of approximately 1 μM (Table 4).

Table 4. Cytotoxicity of 8, 8a, 8b, and 9 toward 3T6 Fibroblast Cells

compd	IC_{50} (μM)
8	40 ± 6% mortality at 200 μM
8a	34.0 ± 0.4
8b	0.98 ± 0.07
9	40 ± 5% mortality at 200 μM

CONCLUSIONS

We have developed a functional screening platform for the identification of selective inhibitors of the bacterial antibiotic-resistance enzyme, R67 DHFR. The platform is based on semiautomated determination of enzymatic activity in the presence of a variety of fragments, or simple compounds similar to the native ligands of the enzyme, to assess inhibition. We observed that a variety of small aromatic compounds offer millimolar range inhibition of R67 DHFR, which is consistent with the proposed "primitive" nature of its relatively promiscuous binding site.[15,39] Weakly inhibiting molecules provided the basis for testing compounds of greater complexity, which provided an increase in affinity from millimolar to micromolar. Importantly, we screened the human DHFR in parallel with R67 DHFR to identify structures with the best prospects for selective inhibition. Thus, we identified a new class of selective, symmetrical, and competitive inhibitors of R67 DHFR (**8** and **9**), which are as potent as congo red but are selective toward R67 DHFR. Compounds **8** and **9** were both based on 1*H*-benzimidazole-5-carboxylic acid (**4**), which had an IC_{50} of 3 mM (Table 1). Joining two benzimidazolecarboxylic acid units into symmetrical structures with a central hydrophobic and flexible linker increased affinity to the low micromolar range. Testing of the analogues **8a** and **8b** demonstrated that carboxylic acid groups and benzimidazoles contribute to affinity. Preliminary cytotoxicity and selectivity experiments demonstrated that **8** and **9** are not highly toxic and thus can serve as lead compounds to develop more potent selective inhibitors of R67 DHFR. We are attempting to gain structural information to determine the mode of binding of the bis-benzimidazole compounds to R67 DHFR, to direct further efforts in discovery and development of selective inhibitors for this emerging drug-resistance target. Future inhibitors should take advantage of the important structural differences between R67 DHFR and human DHFR. In particular, the large size and symmetry of the R67 DHFR active site appears to allow simultaneous binding of two inhibitor molecules in a manner that is not coherent with the narrower, asymmetric active-site cleft of human DHFR.[41] This work provides inspiration for the design of the next generation of inhibitors.

ASSOCIATED CONTENT

Supporting Information

Full list of fragments screened against R67 DHFR, characterization of compounds **8**, **8a**, and **9**, and additional kinetic and molecular docking results. This material is available free of charge via the Internet at http://pubs.acs.org.

AUTHOR INFORMATION

Corresponding Author

*Tel: 514-343-2124. Fax: 514-343-7586. E-mail: joelle.pelletier@umontreal.ca.

Notes

The authors declare no competing financial interest.

ACKNOWLEDGMENTS

We thank the Combinatorial Chemistry Laboratory at l'Université de Montréal and the Medicinal Chemistry Platform at the Institut de Recherche en Immunologie et en Cancérologie (IRIC) de l'Université de Montréal for access to compounds. This work was supported by the Natural Sciences and Engineering Research Council of Canada (NSERC), as well as PROTEO, the Québec Network for Research on Protein Structure, Function and Engineering, and CGCC, the Québec Centre for Green Chemistry and Catalysis, which are funded by les Fonds Québécois pour la Recherche sur la Nature et les Technologies (FQRNT).

ABBREVIATIONS USED

DHFR, dihydrofolate reductase; DHF, dihydrofolate; NADPH, nicotinamide adenine dinucleotide phosphate, reduced form; IC_{50}, concentration giving 50% inhibition; K_i, inhibition constant; CV, column volume; HEPES, 4-(2-hydroxyethyl)-1-piperazineethanesulfonic acid; TMP, trimethoprim; MTT, 3-[4,5-dimethylthiazol-2-yl]-2,5-diphenyltetrazolium bromide; DMEM, Dulbecco's modified Eagle's medium; FBS, fetal bovine serum; LE, ligand efficiency

REFERENCES

(1) Huovinen, P.; Sundstrom, L.; Swedberg, G.; Sköld, O. Trimethoprim and sulfonamide resistance. *Antimicrob. Agents Chemother.* **1995**, *39* (2), 279−289.

(2) (a) Huovinen, P. Resistance to trimethoprim-sulfamethoxazole. *Clin. Infect. Dis.* **2001**, *32* (11), 1608−1614. (b) Forgacs, P.; Wengenack, N. L.; Hall, L.; Zimmerman, S. K.; Silverman, M. L.; Roberts, G. D. Tuberculosis and trimethoprim-sulfamethoxazole. *Antimicrob. Agents Chemother.* **2009**, *53* (11), 4789−4793.

(3) http://www.who.int/selection_medicines/committees/expert/18/applications/Sulfamethoxazole_trimethoprim.pdf (accessed November 29, 2011).

(4) Kehrenberg, C.; Schwarz, S. Trimethoprim resistance in a porcine Pasteurella aerogenes isolate is based on a dfrA1 gene cassette located in a partially truncated class 2 integron. *J. Antimicrob. Chemother.* **2011**, *66* (2), 450−452.

(5) Cabello, F. C. Heavy use of prophylactic antibiotics in aquaculture: A growing problem for human and animal health and for the environment. *Environ. Microbiol.* **2006**, *8* (7), 1137−1144.

(6) Le, T. X.; Munekage, Y.; Kato, S. Antibiotic resistance in bacteria from shrimp farming in mangrove areas. *Sci. Total Environ.* **2005**, *349* (1−3), 95−105.

(7) Segura, P. A.; Garcia-Ac, A.; Lajeunesse, A.; Ghosh, D.; Gagnon, C.; Sauvé, S. Determination of six anti-infectives in wastewater using tandem solid-phase extraction and liquid chromatography-tandem mass spectrometry. *J. Environ. Monit.* **2007**, *9* (4), 307−313.

(8) (a) Burridge, L.; Weis, J. S.; Cabello, F.; Pizarro, J.; Bostick, K. Chemical use in salmon aquaculture: A review of current practices and possible environmental effects. *Aquaculture* **2010**, *306* (1−4), 7−23. (b) Medina, A.; Horcajo, P.; Jurado, S.; De La Fuente, R.; Ruiz-Santa-Quiteria, J. A.; Domínguez-Bernal, G.; Orden, J. A. Phenotypic and Genotypic Characterization of Antimicrobial Resistance in Enterohemorrhagic *Escherichia coli* and Atypical Enteropathogenic *E. coli* Strains from Ruminants. *J. Vet. Diagn. Invest.* **2011**, *23* (1), 91−95. (c) Barlow, R. S.; Pemberton, J. M.; Desmarchelier, P. M.; Gobius, K. S. Isolation and characterization of integron-containing bacteria without antibiotic selection. *Antimicrob. Agents Chemother.* **2004**, *48* (3), 838−842. (d) Zhao, H. X.; Shen, J. Z.; An, X. P.; Fan, H. L.; Cao, J. S.; Li, P. F. Characterization of integrons in multiple antimicrobial resistant *Escherichia coli* isolates from bovine endometritis. *Res. Vet. Sci.* **2011**, *91* (3), 412−414.

(9) Volpato, J. P.; Pelletier, J. N. Mutational 'hot-spots' in mammalian, bacterial and protozoal dihydrofolate reductases associated with antifolate resistance: Sequence and structural comparison. *Drug Resist. Updates* **2009**, *12* (1−2), 28−41.

(10) (a) Plowe, C. V.; Kublin, J. G.; Dzinjalamala, F. K.; Kamwendo, D. S.; Mukadam, R. A.; Chimpeni, P.; Molyneux, M. E.; Taylor, T. E. Sustained clinical efficacy of sulfadoxine-pyrimethamine for uncomplicated falciparum malaria in Malawi after 10 years as first line treatment: five year prospective study. *BMJ* **2004**, *328* (7439), 545. (b) Musset, L.; Pradines, B.; Parzy, D.; Durand, R.; Bigot, P.; Le Bras, J. Apparent absence of atovaquone/proguanil resistance in 477 *Plasmodium falciparum* isolates from untreated French travellers. *J. Antimicrob. Chemother.* **2006**, *57* (1), 110−115.

(11) Appleman, J. R.; Prendergast, N.; Delcamp, T. J.; Freisheim, J. H.; Blakley, R. L. Kinetics of the formation and isomerization of methotrexate complexes of recombinant human dihydrofolate reductase. *J. Biol. Chem.* **1988**, *263* (21), 10304−10313.

(12) Sköld, O. Resistance to trimethoprim and sulfonamides. *Vet. Res.* **2001**, *32* (3−4), 261−273.

(13) (a) Fling, M. E.; Walton, L.; Elwell, L. P. Monitoring of plasmid-encoded, trimethoprim-resistant dihydrofolate reductase genes: Detection of a new resistant enzyme. *Antimicrob. Agents Chemother.* **1982**, *22* (5), 882−888. (b) Stone, D.; Smith, S. L. The amino acid sequence of the trimethoprim-resistant dihydrofolate reductase specified in *Escherichia coli* by R-plasmid R67. *J. Biol. Chem.* **1979**, *254* (21), 10857−10861.

(14) Alonso, H.; Gready, J. E. Integron-sequestered dihydrofolate reductase: A recently redeployed enzyme. *Trends Microbiol.* **2006**, *14* (5), 236−242.

(15) Holland, J. C.; Linn, C. E.; DiGiammarino, E.; Nichols, R.; Howell, E. E. Does R67 dihydrofolate reductase possess a proton donor? *Adv. Exp. Med. Biol.* **1993**, *338*, 493−498.

(16) Huovinen, P. Trimethoprim resistance. *Antimicrob. Agents Chemother.* **1987**, *31* (10), 1451−1456.

(17) Howell, E. E. Searching sequence space: two different approaches to dihydrofolate reductase catalysis. *ChemBioChem* **2005**, *6* (4), 590−600.

(18) Schmitzer, A. R.; Lépine, F.; Pelletier, J. N. Combinatorial exploration of the catalytic site of a drug-resistant dihydrofolate reductase: Creating alternative functional configurations. *Protein Eng. Des. Sel.* **2004**, *17* (11), 809−819.

(19) Krahn, J. M.; Jackson, M. R.; DeRose, E. F.; Howell, E. E.; London, R. E. Crystal structure of a type II dihydrofolate reductase catalytic ternary complex. *Biochemistry* **2007**, *46* (51), 14878−14888.

(20) (a) Zartler, E. R.; Shapiro, M. J. Fragonomics: Fragment-based drug discovery [Review]. *Curr. Opin. Chem. Biol.* **2005**, *9* (4), 366−370. (b) de Kloe, G. E.; Bailey, D.; Leurs, R.; de Esch, I. J. Transforming fragments into candidates: Small becomes big in medicinal chemistry. *Drug Discovery Today* **2009**, *14* (13−14), 630−646. (c) Gozalbes, R.; Carbajo, R. J.; Pineda-Lucena, A. Contributions of computational chemistry and biophysical techniques to fragment-based drug discovery. *Curr. Med. Chem.* **2010**, *17* (17), 1769−1794.

(21) Murray, C. W.; Rees, D. C. The rise of fragment-based drug discovery. *Nat. Chem.* **2009**, *1* (3), 187−192.

(22) Blakley, R. L. Crystalline Dihydropteroylglutamic Acid. *Nature* **1960**, *188*, 231−232.

(23) Mayence, A.; Pietka, A.; Collins, M. S.; Cushion, M. T.; Tekwani, B. L.; Huang, T. L.; Eynde, J. J. V. Novel bisbenzimidazoles with antileishmanial effectiveness. *Bioorg. Med. Chem. Lett.* **2008**, *18* (8), 2658−2661.

(24) Donahoe, H. B.; Benjamin, L. E.; Fennoy, L. V.; Greiff, D. Synthesis of Potential Rickettsiostatic Agents.1a I. 4,4′-Dicarboxy-α,ι-diphenoxyalkanes1b. *J. Org. Chem.* **1961**, *26* (2), 474−476.

(25) Yachnin, B. J.; Colin, D. Y.; Volpato, J. P.; Ebert, M.; Pelletier, J. N.; Berghuis, A. M. Novel crystallization conditions for tandem variant R67 DHFR yield a wild-type crystal structure. *Acta Crystallogr., Sect. F: Struct. Biol. Cryst. Commun.* **2011**, *67*, 1316−1322.

(26) Schägger, H.; von Jagow, G. Tricine-sodium dodecyl sulfate-polyacrylamide gel electrophoresis for the separation of proteins in the range from 1 to 100 kDa. *Anal. Biochem.* **1987**, *166* (2), 368−379.

(27) Volpato, J. P.; Yachnin, B. J.; Blanchet, J.; Guerrero, V.; Poulin, L.; Fossati, E.; Berghuis, A. M.; Pelletier, J. N. Multiple conformers in active site of human dihydrofolate reductase F31R/Q35E double mutant suggest structural basis for methotrexate resistance. *J. Biol. Chem.* **2009**, *284* (30), 20079−20089.

(28) Park, H. Y.; Zhuang, P.; Nichols, R.; Howell, E. E. Mechanistic studies of R67 dihydrofolate reductase - Effects of pH and an H62C mutation. *J. Biol. Chem.* **1997**, *272* (4), 2252−2258.

(29) Chopra, S.; Dooling, R. M.; Horner, C. G.; Howell, E. E. A Balancing Act between Net Uptake of Water during Dihydrofolate Binding and Net Release of Water upon NADPH Binding in R67 Dihydrofolate Reductase. *J. Biol. Chem.* **2008**, *283* (8), 4690−4698.

(30) Cheng, Y.; Prusoff, W. H. Relationship between the inhibition constant (K1) and the concentration of inhibitor which causes 50% inhibition (I50) of an enzymatic reaction. *Biochem. Pharmacol.* **1973**, *22* (23), 3099−3108.

(31) Thomsen, R.; Christensen, M. H. MolDock: a new technique for high-accuracy molecular docking. *J. Med. Chem.* **2006**, *49* (11), 3315−3321.

(32) Trott, O.; Olson, A. J. AutoDock Vina: Improving the speed and accuracy of docking with a new scoring function, efficient optimization, and multithreading. *J. Comput. Chem.* **2010**, *31* (2), 455−461.

(33) Mosmann, T. Rapid colorimetric assay for cellular growth and survival: Application to proliferation and cytotoxicity assays. *J. Immunol. Methods* **1983**, *65* (1−2), 55−63.

(34) Hicks, S. N.; Smiley, R. D.; Hamilton, J. B.; Howell, E. E. Role of ionic interactions in ligand binding and catalysis of R67 dihydrofolate reductase. *Biochemistry* **2003**, *42* (36), 10569−10578.

(35) Kakkar, T.; Boxenbaum, H.; Mayersohn, M. Estimation of Ki in a competitive enzyme-inhibition model: Comparisons among three methods of data analysis. *Drug Metab. Dispos.* **1999**, *27* (6), 756−762.

(36) Smiley, R. D.; Stinnett, L. G.; Saxton, A. M.; Howell, E. E. Breaking symmetry: mutations engineered into R67 dihydrofolate reductase, a D2 symmetric homotetramer possessing a single active site pore. *Biochemistry* **2002**, *41* (52), 15664−15675.

(37) Bradrick, T. D.; Beechem, J. M.; Howell, E. E. Unusual binding stoichiometries and cooperativity are observed during binary and ternary complex formation in the single active pore of R67 dihydrofolate reductase, a D2 symmetric protein. *Biochemistry* **1996**, *35* (35), 11414−11424.

(38) Alonso, H.; Gillies, M. B.; Cummins, P. L.; Bliznyuk, A. A.; Gready, J. E. Multiple ligand-binding modes in bacterial R67 dihydrofolate reductase. *J. Comput.-Aided Mol. Des.* **2005**, *19* (3), 165−187.

(39) Howell, E. E.; Shukla, U.; Hicks, S. N.; Smiley, R. D.; Kuhn, L. A.; Zavodszky, M. I. One site fits both: A model for the ternary complex of folate + NADPH in R67 dihydrofolate reductase, a D2 symmetric enzyme. *J. Comput.-Aided Mol. Des.* **2001**, *15* (11), 1035−1052.

(40) Segel, I. H. In *Enzyme Kinetics: Behavior and Analysis of Rapid Equilibrium and Steady-State Enzyme Systems*, Wiley Classics Library ed.; John Wiley and Sons: New York, 1993; p 957.

(41) Oefner, C.; D'Arcy, A.; Winkler, F. K. Crystal structure of human dihydrofolate reductase complexed with folate. *Eur. J. Biochem.* **1988**, *174* (2), 377−385.